HHS Public Access

Author manuscript

J Med Chem. Author manuscript; available in PMC 2016 January 20.

Published in final edited form as:

J Med Chem. 2015 March 12; 58(5): 2290–2298. doi:10.1021/jm501751b.

Exploitation of the Ability of γ-Tocopherol to Facilitate Membrane Co-localization of Akt and PHLPP1 to Develop PHLPP1-Targeted Akt Inhibitors

Ribai Yan[†], **Hsiao-Ching Chuang**[†], **Naval Kapuriya**[‡], **Chih-Chien Chou**[†], **Po-Ting Lai**[†], **Hsin-Wen Chang**[§], **Chia-Ning Yang**[§], **Samuel K. Kulp**[†], and **Ching-Shih Chen**[†,∥,*]

[†]Division of Medicinal Chemistry and Pharmacognosy, College of Pharmacy and Comprehensive Cancer Center, The Ohio State University, Columbus, Ohio 43210, United States

[‡]Department of Chemistry, Shree M. & N. Virani Science College, Saurashtra University, Rajkot 360 005, Gujarat India

[§]Institute of Biotechnology, National University of Kaohsiung, 811 Kaohsiung, Taiwan

[∥]Institute of Biological Chemistry, Academia Sinica, Nankang, 115 Taipei, Taiwan

Abstract

Previously, we reported that Akt inactivation by γ-tocopherol (**2**) in PTEN-negative prostate cancer cells resulted from its unique ability to facilitate membrane co-localization of Akt and PHLPP1 (PH domain leucine-rich repeat protein phosphatase isoform 1), a Ser473-specific Akt phosphatase, through pleckstrin homology (PH) domain binding. This finding provided a basis for exploiting **2** to develop a novel class of PHLPP1-targeted Akt inhibitors. Here, we used **3** (γ-VE5), a side chain-truncated **2** derivative, as a scaffold for lead optimization. The proof-of-concept of this structural optimization was obtained by **20**, which exhibited higher antitumor efficacy than **3** in PTEN-negative cancer cells through PHLPP1-facilitated Akt inactivation. Like **3, 20** preferentially recognized the PH domains of Akt and PHLPP1, as its binding affinities for other PH domains, including those of ILK and PDK1, were an order-of-magnitude lower. Moreover, **20** was orally active in suppressing xenograft tumor growth in nude mice, which underlines the translational potential of this new class of Akt inhibitor in PTEN-deficient cancers.

Graphical abstract

[*]**Corresponding Author**. Phone: 614-688-4008. chen.844@osu.edu. Address: College of Pharmacy, The Ohio State University, 500 West 12th Avenue, Parks Hall, Room 336, Columbus, Ohio 43210, United States.

R.Y. and H.C.C. contributed equally to this manuscript.

ASSOCIATED CONTENT

Supporting Information

Synthetic procedures and pertinent spectroscopic data for **4–22** and synthetic intermediates, and NMR spectra of all compounds. This material is available free of charge via the Internet at http://pubs.acs.org.

Author Contributions

The manuscript was written through contributions from all authors. All authors have given approval of the final version of the manuscript.

The authors declare no competing financial interest.

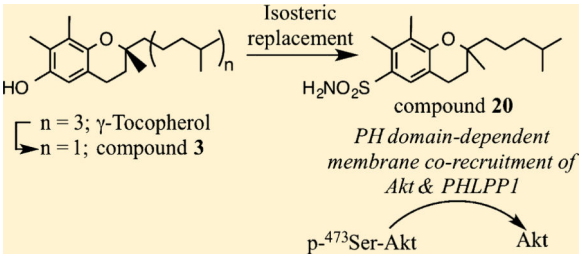

INTRODUCTION

It is well recognized that dysregulated phosphoinositol-3-kinase (PI3K)/Akt signaling through phosphatase and tensin homologue (PTEN) mutations is an important driver of oncogenesis and tumor progression in many types of cancer.[1,2] The Akt signaling pathway is initiated by the recruitment of Akt by phosphatidylinositol (3,4,5)-trisphosphate (PIP_3), a PI3K product, to the cell membrane where it is phosphorylated at Thr308 and Ser473 by phosphoinositide-dependent kinase (PDK)1 and PDK2, respectively.[3,4] Upon activation, Akt is involved in the regulation of cell growth and survival, translation, protein synthesis/degradation, and cell metabolism through a plethora of downstream effectors, including mTOR, glycogen synthase kinase, murine double minute 2 (MDM2), inhibitor of nuclear factor κB kinase (IKK), and Foxo3a. In light of the pivotal role of Akt in cancer biology,[5] development of small-molecule Akt inhibitors has received considerable attention in the past decade.[6,7] To date, a wide array of Akt inhibitors with distinct mechanisms have been developed, including those targeting the ATP-binding pocket,[8–10] kinase domain,[11,12] hinge region,[12–16] or PIP_3-binding pleckstrin homology (PH) domain,[17–24] some of which are currently in clinical trials in patients with different types of malignancies.[6]

In the course of our investigation of the mechanism whereby vitamin E suppresses cancer cell proliferation, we demonstrated that α-tocopherol (**1**) and, to a greater extent, γ-tocopherol (**2**), can mediate the site-specific dephosphorylation of Akt at Ser473 with activities paralleling their respective antiproliferative potencies in PTEN-negative prostate cancer cells.[25] We obtained evidence that this selective Akt dephosphorylation is attributable to the unique ability of **1** and **2** to facilitate the membrane co-localization of Akt and PH domain leucine-rich repeat protein phosphatase 1 (PHLPP1), a Ser473-specific Akt protein phosphatase,[26–28] through interactions of the chroman ring in the polar headgroup with the PH domain of these proteins (Figure 1A).

Recent evidence suggests that PHLPP1 forms a tumor suppressor network with PTEN in regulating Akt signaling, and that, upon loss of PTEN, PHLPP1 acts as a brake to counteract PTEN deficiency-induced Akt activation.[29] Thus, PHLPP1 activation represents a therapeutically relevant target for PTEN mutant tumors. From a mechanistic perspective, the unique ability of **1** and **2** to induce PHLPP1-mediated Akt dephosphorylation suggests that PHLPP1 is a “druggable” target, which provides a molecular rationale for the pharmacological exploitation of **2** to develop a novel class of PHLPP1-targeted Akt inhibitors.

Consequently, we developed **3** [(*S*)-2,7,8-trimethyl-2-(4-methylpentyl)chroman-6-ol] (γ-VE5) (Figure 1A) by removing two isoprenyl units from the aliphatic side chain of **2**,[25] which increased the membrane association of Akt and PHLPP1. We obtained evidence that this PHLPP1-mediated Akt inhibition underlies the in vitro and/or in vivo efficacy of **3** in suppressing the proliferation of PTEN-negative LNCaP and PC-3 prostate cancer cells.[25] Here, we describe the use of **3** to conduct lead optimization to develop a novel class of PHLPP1-targeted Akt inhibitors, of which the proof-of-concept was obtained by the structurally optimized derivative **20**. The mode of action of these Akt inhibitors is conceptually distinct from that of PH domain-targeted inhibitors,[17–21] and thus represents a novel approach for the design of new Akt inhibitors. From a translational perspective, this new class of agents provides a proof-of-concept that PHLPP1 activation is a druggable target.

RESULTS

Structural Optimization of 3

Previously, we proposed a mechanism of action for **3** in which the phytyl side chain plays a role in mediating membrane anchorage, while the chroman moiety binds the target proteins at the membrane–cytoplasm interface.[25] Accordingly, we rationalized that the ability of **3** to facilitate the membrane association of PHLPP1 and Akt could be enhanced by modifying the chroman substructure. Docking of **3** into the Akt PH domain (PDB code, 1H10) revealed that **3** interacted with the binding pocket within the variable loop VL2 through hydrogen bonding between the phenolic OH and the peptide backbone of Ala50-Leu52 (Figure 1B).[25] Because the phytyl side chain is not involved in ligand recognition, the binding of **3** should be independent of its stereochemical configuration. This premise was borne out by the finding that the binding affinity of the racemic form of **3** (**4**; Figure 1C) for the Akt PH domain was identical to that of **3**. Surface plasmon resonance (SPR) spectroscopy revealed that the dissociation constants (K_d) for **3** and **4** were 0.54 ± 0.24 and 0.52 ± 0.18 μM, respectively (Table 1). Moreover, the antiproliferative activity of **4** against LNCaP cells remained unchanged as compared to its chiral counterpart (IC_{50}, 7.8 versus 7.5 μM; Table 1), indicating that cell permeability and antiproliferative activity were independent of the chirality of the side chain. Consequently, a series of derivatives of **3** with modifications of the chroman ring were synthesized (Figure 1C) and evaluated for lipophilicity, binding affinity for the Akt-PH domain, and antiproliferative activity against LNCaP prostate cancer cells (Table 1).

Consistent with the pivotal role of hydrogen bonding in ligand recognition, PH domain binding was abolished by masking the phenolic –OH of **4** with a methyl function (**5**, Figure 1C; K_d, 8.5 ± 2.7 μM, Table 1), leading to loss of antitumor activity. Moreover, evidence suggests that the C-7 and C-8 methyl substituents on the chroman headgroup were not required for PH domain binding as **6** and **7**, the C-7 demethylated and C-7,8-bis-demethylated derivatives of **4**, respectively, exhibited modest increases in binding affinity (K_d, 0.41 ± 0.12 and 0.35 ± 0.10 μM, respectively). This increased binding affinity was likely attributable to reduced lipophilicity of **6** and **7** relative to **3**, as suggested by a positive correlation between K_d and calculated log *P* values (cLogP: **3**, 5.8; **6**, 5.3; **7**, 4.8; Table 1). In

principle, this reduced lipophilicity might favor ligand binding within a hydrophilic microenvironment in the binding pocket, which, however, did not give rise to parallel increases in antiproliferative efficacy (IC_{50}: **6**, 7.5 μM; **7**, 10 μM). As **3**, and presumably its derivatives, facilitate Ser473-Akt dephosphorylation through the membrane co-localization of Akt and PHLPP1,[25] this discrepancy underscored the complex physicochemical dynamics governing ligand–protein recognition at the membrane–cytoplasm interface. For example, in a homogeneous, liquid-phase system, improved binding affinities are often associated with improved biological responses. However, for ligands acting at the membrane–cytoplasm interface, the biological response might be affected by a ligand's polarity to the extent that it affects partitioning between membrane and cytoplasm. While increased polarity could facilitate interaction of ligand with cytoplasmic proteins, it may interfere with its association with the membrane and thus mitigate biological response. To shed light onto this issue, we compared the PH domain binding affinities and antiproliferative activities of **4, 6**, and **7** to those of their respective 4-keto derivatives **8, 9**, and **10**. With increased polarity, **8, 9**, and **10** (cLogP: 4.9, 4.1, and 3.6, respectively) exhibited increased binding affinities for the Akt PH domain (K_d, 0.41 ± 0.18, 0.32 ± 0.12, and 0.28 ± 0.10 μM, respectively) as compared to **4, 6**, and **7**, respectively (Table 1). Despite this increased binding affinity, there was a sharp drop in the antiproliferative activities of **9** and **10** (IC_{50}, 18 and >30 μM, respectively) relative to **6** and **7**, respectively. This dichotomy is consistent with the aforementioned proposed mode of action of these PHLPP1-targeted Akt inhibitors in which association with the membrane is required to facilitate the localization of target proteins to the membrane (see the following section Mechanistic Validation for more discussion).

To further understand the SAR, we used **6** as a platform for modifications by substituting the C-8 methyl moiety with various functional groups, including $–CF_3$ (**11**; cLogP, 5.7), –OH (**12**; cLogP, 4.6), $–OCH_3$ (**13**; cLogP, 4.9), –F (**14**; cLogP, 5.0), and –Br (**15**; cLogP, 5.6) (Figure 1C). Consistent with our premise, as the lipophilicity of **11, 14**, and **15** was similar to that of **6**, these derivatives showed comparable K_d and IC_{50} values (Table 1). Nevertheless, replacement of $–CH_3$ with –OH (**12**) or $–OCH_3$ (**13**) resulted in a substantial loss of activities in both binding and cell killing, indicating incompatibility of these substitutions with the binding pocket.

To further probe the hydrophilic surface involved in ligand recognition inside the binding pocket, we synthesized a series of derivatives for biological evaluation, including those containing permuted –OH substitutions (**16** and **17**), the 3,4-dihydro-2*H*-quinoline core (**18**), and 6-NH_2 substitution (**19**). With respect to the phenolic –OH, a C-6 → C-5 shift in **10** or C-6 → C-7 shift in **12** had no apparent effect on binding affinity or antitumor activity in the resulting congeners, **16** (K_d, 0.34 ± 0.15 μM; IC_{50}, 11 μM) and **17** (K_d, 0.98 ± 0.3 μM; IC_{50}, 23 μM). It is noteworthy that **18** exhibited an order-ofmagnitude increase, relative to **6**, in binding affinity for the Akt PH domain (K_d, 0.03 ± 0.02 versus 0.41 ± 0.12 μM). In accordance with the docking data (Figure 1B), this differential binding reflected differences between the ether oxygen versus the basic nitrogen atom in interacting with the electropositive surface in the binding pocket (Figure 1B). This increased binding of **18**, however, did not lead to a parallel increase in antiproliferative activity (IC_{50}, 10 μM),

confirming an intricate relationship between the hydrophilicity of the ligand and its mode of action at the membrane–cytoplasm interface.

On the basis of the above SAR data, **4, 14**, and **15** were selected to conduct a second-tier of modifications through isosteric replacement of the phenolic –OH with a sulfonamide function in light of its greater hydrogen bonding potential and metabolic stability. This modification was accompanied by increased polarity as indicated by lower clogP values of the resulting compounds (Table 1; **20**, 4.8; **21**, 4.0; **22**, 4.5). As shown, this conversion of **4** and **15** led to at least a 2-fold increase in the Akt PH domain binding affinity and the in vitro antiproliferative efficacy in the resulting compounds **20** (K_d, 0.20 ± 0.08 μM; IC_{50}, 3 μM) and **22** (K_d, 0.22 ± 0.10 μM; IC_{50}, 4.5 μM), respectively. However, **21** behaved differently as this isosteric replacement resulted in substantial loss of antiproliferative efficacy relative to **14** (IC_{50}, 20 versus 9 μM), although binding affinity for Akt PH domain remained unchanged (K_d, **14**, 0.34 ± 0.16 μM; **21**, 0.35 ± 0.12 μM). Again, we suggest that this discrepancy is associated with differences in hydrophilicity, which may have implications for biological activity through effects on membrane association.

The differential antitumor activities of these sulfonamide derivatives vis-à-vis **3** were also examined in another PTEN-negative cell line, PC-3, in which **5** was used as negative control. As shown, PC-3 cells were equally susceptible to the antiproliferative effects of these derivatives, as the IC_{50} values were virtually identical to those determined in LNCaP cells, while **5** remained inactive (Figure 2A, left). Compared to prostate cancer cells, normal prostate epithelial cells (PrECs) were resistant, with respective IC_{50} values that were 3-fold higher than that in LNCaP or PC-3 cells (Figure 2A, right).

Mechanistic Validation of the Mode of Action of 20 and 22 in Facilitating PHLPP1-Targeted Akt Inhibition

To investigate whether the sulfonamide derivatives retained the ability of **3** to facilitate PHLPP1-mediated Akt inhibition, we examined the effects of these sulfonamides vis-à-vis **3** on Akt signaling in LNCaP and PC-3 cells. Cells were exposed to individual compounds at different concentrations for 24 h, and the phosphorylation status of Akt and/or its downstream substrates MDM2 and IKK were examined by Western blotting. As shown, **3, 20**, and **22** dose-dependently reduced the phosphorylation level of Akt and/or MDM2 and IKK in both cell lines (Figure 2B), with relative potencies paralleling the binding affinities to the Akt PH domain binding. Consistent with the involvement of PHLPP1 in this effect, drug-induced Akt dephosphorylation was highly specific for Ser473, as no changes at the Thr308 site were noted.

In contrast, **21** failed to elicit Ser473-Akt dephosphorylation, which was reflected in its low antiproliferative activity (Table 1) despite its ability to bind the Akt PH domain. We hypothesized that this discrepancy might be related to the aforementioned proposed effect of reduced lipophilicity on the ligand's interaction with the membrane. Specifically, the hydrophilic nature of **21**, as well as that **9** and **10** as aforementioned, might interfere with their abilities to mediate co-localization of target proteins at the membrane–cytoplasm interface.

This premise was borne out by the immunocytochemical analysis of the effects of these three sulfonamide derivatives versus **3** and DMSO on the cellular distribution of Akt and PHLPP1 in LNCaP cells. Similar to **3** (10 μM), **20** and **22**, each at 5 μM, facilitated the localization of Akt and PHLPP1 to the plasma membrane. Immunofluorescence staining (Figure 3A) and cross-sectional analysis of fluorescence intensities, represented as three-dimensional surface plots (Figure 3B), show that, while Akt and PHLPP1 were diffusely distributed in the cytoplasm, nucleus, and plasma membrane of vehicle-treated cells, these proteins responded to **20** and **22** by localizing to cell membranes. In contrast, **21** (10 μM) caused no change in the cellular distribution of Akt or PHLPP1 relative to vehicle control. This inability to elicit PH domain-mediated membrane localization suggests that **21** might not be membrane-associated due to its increased polarity.

The effect of **20** on the membrane co-localization of Akt and PHLPP1, a characteristic feature of **3**,[25] was further validated by two lines of evidence. Western blot analysis of the membrane versus cytoplasmic fractions of drug-treated LNCaP cells showed that **20** displayed higher potency than **3** in facilitating the membrane translocation of these two target proteins in a dose-dependent manner (Figure 4A). Equally important, this increased membrane association was accompanied by parallel decreases in the abundance of cytoplasmic Akt and PHLPP1 and the phosphorylation of Ser473-Akt in both cellular fractions. Consistent with this finding, subsequent immuno-precipitation analysis of Akt-PHLPP1 complexes from the membrane fraction revealed dose-dependent increases in the association of these two proteins in **3**-, and to a greater extent, **20**-treated cells (Figure 4B). Together, these data validate the integral role of membrane localization of Akt and PHLPP1 in **20**-facilitated Ser473-Akt dephosphorylation.

Membrane Localization of Akt and PHLPP1 by 20 and 22

Previously, we demonstrated that **3** displayed a high degree of specificity in recognizing the PH domain of Akt and PHLPP1 as the respective binding affinities were an order-of-magnitude greater than those for the PH domains of other PH domain-containing proteins, including PDK1 and integrin-linked kinase (ILK).[25] Pursuant to this finding, we measured the binding affinities of **20** and **22** vis-à-vis **3** for the PH domain of PHLPP1, PDK1, and ILK by SPR spectroscopy. Although **20** and **22** exhibited higher binding affinities than **3** for the PH domain of Akt (Table 1), the respective K_d values for the PH domain of PHLPP1 remained unchanged (Table 2). Nevertheless, the binding affinities of these two compounds for the PH domains of PDK1 and ILK were 8.6–27 times lower than those for Akt and PHLPP1 (Table 2), which underscores the preferentially binding of these two derivatives to the PH domains of Akt and PHLPP1 relative to PDK1 and ILK. To confirm this finding, we assessed the impact of **20** on the intracellular distribution of endogenous ILK in LNCaP cells by immunocytochemistry. In contrast to Akt and PHLPP1, no apparent changes in the distribution of ILK were noted in response to **20** relative to control (Figure 4C).

In Vivo Efficacy of 20 versus 3 in Suppressing PC-3 Xenograft Tumor Growth

Pursuant to the above findings, the effect of **20** vis-à-vis **3** on tumor growth in vivo was compared in athymic nude mice bearing subcutaneous PC-3 xenograft tumors. Consistent with our previous report,[25] daily intraperitoneal injection of **3** significantly suppressed PC-3

xenograft tumor growth relative to vehicle-treated control (*$P < 0.05$; Figure 5A, left panel). This in vivo efficacy, however, was not apparent when **3** was orally administered via gavage (Figure 5B, left panel).

In contrast to **3**, which was not orally active, **20** was equipotent in suppressing PC-3 tumor growth irrespective of the route of administration (*$P < 0.05$ relative to vehicle control in both cases). Moreover, Western blot analysis of tumor lysates showed that this tumor-suppressive activity correlated with the ability to block Akt signaling, as manifested by parallel decreases in the phosphorylation levels of Akt, MDM2, and IKK (Figure 5A,B, middle and right panels). Consistent with the role of PHLPP1 in mediating this drug-induced Akt dephosphorylation, no apparent change in Thr308-Akt phosphorylation was noted. In contrast, orally administered **3** was unable to affect any of these signaling markers and thus had no in vivo tumor-suppressive activity.

DISCUSSION

On the basis of our novel finding that the PH domains of Akt and the Akt-specific protein phosphatase PHLPP1 represent major antitumor targets of **2** in PTEN-negative cancer cells,[25] we report in this study the use of **3**, a side chain-truncated derivative of **2**, to develop a novel class of PHLPP1-targeted Akt inhibitors. The proof-of-concept was provided by **20**, which exhibited increased binding affinity for the Akt PH domain and antiproliferative activity relative to **3**, retained the ability to induce the PH domain-dependent co-localization of Akt and PHLPP to the membrane with consequent dephosphorylation of Akt at S473 and, in contrast to **3**, was orally active in suppressing xenograft tumor growth. As opposed to the –OH function in **3**, the sulfonamide moiety of **20** might bestow desirable pharmacokinetic properties by conferring improved oral absorption, as well as protection against oxidation and metabolic transformation in vivo. Moreover, in vitro and in vivo biomarkers correlated the tumor-suppressive activity of **20** with its on-target effect on Akt signaling. This unique mode of action in activating the tumor-suppressive function of PHLPP1 to inactivate Akt through membrane co-localization is distinct from that of the previously reported Akt PH domain inhibitors that block the membrane translocation of Akt by interfering with its interaction with PIP_3.[17–24]

From a mechanistic perspective, our finding that compounds **3, 20**, and **22** exhibited differential binding to the PH domains of Akt and PHLPP1 relative to those of PDK1 and ILK (Table 2) argue against a general, bulk effect of these compounds on membrane properties, such as phase partitioning, “fluidity,” curvature, or packing stresses. We hypothesized that these tocopherol-derived Akt inhibitors facilitated the membrane association of Akt and PHLPP1 through interactions with both plasma membrane and the target proteins. However, in light of the complex, dynamic behavior of ligands within membranes and how it might influence ligand–protein interactions at the membrane–cytoplasm interface, the mechanism by which **3, 20**, and **22** interact with the membrane and Akt and PHLPP1 to elicit their co-localization at the cell membrane warrants further clarification.

Although the tumor suppressor role of PHLPP1 has been well recognized, the cellular mechanism by which PHLPP1 is activated remains unclear. Nonetheless, this new class of agents provides a proof-of-concept that PHLPP1 is a druggable target. As this PHLPP1-targeted Akt inhibition appears to take place at the membrane–cytoplasmic interface, we postulate that this new class of inhibitors requires unique physicochemical properties that allow their membrane association. Although Lipinski's rule of five indicates that the lipophilicity of drug-like compounds, as expressed by log *P*, should be less than 5,[30] our SAR analysis indicates a more complicated relationship between lipophilicity and biological activity, such that the antitumor activity might be lost consequent to increased polarity despite greater binding affinity for the target proteins. In the context of "drug-like" features, this membrane-associated drug action might prove advantageous. For example, our previous findings suggest that these Akt inhibitors may achieve high concentrations in local nonraft regions of cytoplasmic membranes to mediate their antitumor effect, as they preferentially facilitated the accumulation of Akt in these nonraft domains.[25] Equally important, association with membranes could limit exposure of these agents to cytosolic proteins, which therefore might reduce off-target effects due to nonspecific interactions with intracellular proteins.

An issue that warrants discussion is how **20** could compete with PIP_3 for Akt binding in light of the three orders-of-magnitude difference between the binding affinity of PIP_3 and that of **20** for Akt (nM versus sub-μM, respectively). Previously, we demonstrated that this **3**-induced membrane accumulation and dephosphorylation of Akt occurs in nonraft microdomains,[25] which contrasts with PIP_3-induced membrane recruitment and activation of Akt which occurs in cholesterol-rich lipid rafts.[31,32] On the basis of this finding, we rationalize that **20** might counteract the effect of PIP_3-mediated Akt activation in PTEN-negative cancer cells through differential recruitment of phospho-Akt to distinct regions of the plasma membrane. As shown by immunofluorescent staining, most Akt in LNCaP cells is localized to the cytoplasm despite elevated PIP_3 levels (Figure 3), which is consistent with the notion that Akt, after being phosphorylated, is released into the cytoplasmic/nuclear compartment to mediate its biological functions. We postulate that this cytoplasmic pool of phospho-Akt, along with PHLPP1, was responsive to **20**-mediated membrane recruitment to nonraft domains, leading to PHLPP1-mediated Akt dephosphorylation.

Relative to **3**, the improved efficacy of **20** in facilitating Akt dephosphorylation was attributable to increased binding affinity for the PH domain of Akt, while that for PHLPP1 remained unaltered. Evidence suggests that **20** retained the ability of **3** to preferentially bind the PH domains of Akt and PHLPP1 over that of PDK1 and ILK. While the structure of the PHLPP1 PH domain remains undefined, we previously attributed this differential binding to differences in the secondary structure between the Akt VL2 loop and homologous sequences in other PH domains [Akt, ^{38}YKERPQDVDQREAPL^{52}; PDK1, ^{487}VDPVNKVLKGEIPWSQ^{502}; ILK, ^{198}KLNENHSGELWKGRW^{212}].[25] Specifically, the PH domains of PDK1 and ILK contain a β sheet structure in lieu of a variable loop structure, which might underlie the ability of **20** to differentially recognize different PH domain-containing proteins.

CONCLUSION

By exploiting the unique ability of **2** to facilitate Akt dephosphorylation through PH domain-mediated membrane co-localization of Akt and PHLPP1, this study describes the development of a novel class of PHLPP1-targeted Akt inhibitors, of which the proof-of-concept was obtained with **20**. This unique mode of action provides a new concept for the design of Akt inhibitors, which might foster new therapeutic strategies for PTEN-negative cancers.

EXPERIMENTAL SECTION

Chemistry

Detailed information on the syntheses of **4** to **22** is described in the Supporting Information. Compound **3** was synthesized as previously reported.[25] The purities of all tested compounds were determined to be >95% by a Hitachi Elite LaChrom HPLC system (comprising a Versa Grad Prep 36 pump, an L-2400 UV detector, an L-2200 auto sampler, and a 250 mm × 4.6 mm Phenomenex Luna 5 μ C18 column).

Cell Lines, Culture, Reagents, and Antibodies

The prostate cancer cell lines, LNCaP and PC-3, were purchased from American Type Culture Collection (Manassas, VA) and maintained in RPMI 1640 medium containing 10% fetal bovine serum at 37 °C in a humidified incubator containing 5% CO_2. For experiments, LNCaP cells were plated on poly-L-lysine-coated culture flasks at a density of 12000 cells per cm^2 surface area for 24 h, followed by treatment with test agents in serum-free RPMI 1640 medium. 3-(4,5-dimethylthiazol-2-yl)-2,5-diphenyl-2*H*-tetrazolium bromide (MTT) was obtained from TCI America (Portland, OR) and the ECL western blotting system from GE Healthcare Life Sciences (Pittsburgh, PA). Antibodies specific for the following protein targets were used: phospho-S473-Akt, phospho-T308-Akt, Akt, PDK-1, and β-actin (Cell Signaling Technology, Inc., Beverly, MA), PHLPP (Novus Biologicals, Littleton, CO), and Na^+-K^+ ATPase and ILK (Santa Cruz Biotechnology, Inc., Santa Cruz, CA). Alexa Fluor 555- and 488-conjugated goat antirabbit and antimouse IgG were purchased from Invitrogen (Carlsbad, CA), and antimouse and antirabbit secondary antibodies was obtained from Jackson ImmunoResearch Laboratories (West Grove, PA).

Cell Viability Assay

LNCaP cells were plated into poly-L-lysinecoated 96-well plates and PC-3 cells into uncoated plates at the density of 5000 cells per well in the presence of 10% FBS. Exposure to test agents in serum-free medium was initiated 24 h later. After 24 h of treatment, cells were incubated with MTT (0.5 mg/mL, final concentration) for an additional 2 h. The medium was then removed from each well and replaced with DMSO to dissolve the reduced MTT dye for subsequent colorimetric measurement of absorbance at 595 nm. Cell viabilities are expressed as percentages of that in the corresponding vehicle-treated control group.

Surface Plasmon Resonance Spectroscopy

Binding experiments were performed using a Biacore T100 system (GE Healthcare, Piscataway, NJ). The GST-tagged PH domain fusion protein of Akt, PHLPP1, PDK1, or ILK was immobilized on a CM5 S sensor chip using Biacore's Amine Coupling Kit to a level of 17000 response units. Compounds at concentrations ranging from 1 to 20 μM were injected at a high flow rate (30 μL/min) over the biosensor surface for binding analyses. DMSO concentrations in all samples and running buffer were 1% (v/v) or less. Data were analyzed using Biacore T100 evaluation software.

Cell Lysis and Immunoblotting

Cells were exposed to the test agents in 10 cm dishes and then collected by scraping. The cell pellets were washed once with PBS and then lysed in SDS lysis buffer containing 50 mM Tris-HCl (pH 8), 10 mM EDTA, 1% SDS, and a commercial protease inhibitor cocktail (2 mM AEBSF, 1 mM EDTA, 130 μM bestatin, 14 μM E-64, 1 μM leupeptin, 0.3 μM aprotinin). After centrifugation of lysates for 20 min at 14000*g*, the supernatants were collected. One μL of each supernatant was used for determination of protein concentration using a colorimetric bicinchoninic assay (Pierce, Rockford, IL), and to the remaining sample was added an equal volume of 2× SDS-polyacrylamide gel electrophoresis sample loading buffer (62.5 mM Tris-HCl, pH 6.8, 4% SDS, 5% β-mercaptoethanol, 20% glycerol, 0.1% bromophenol blue), followed by incubation in boiling water for 5 min. Equivalent amounts of proteins were resolved in SDS-polyacrylamide gels and then transferred to nitrocellulose membranes using a semidry transfer cell. The transblotted membrane was washed twice with Tris-buffered saline containing 0.1% Tween 20 (TBST). After blocking with TBST containing 5% nonfat milk for 40 min, the membrane was incubated with the appropriate primary antibody (1:1000) in TBST-1% nonfat milk at 4 °C overnight. The membrane was then washed three times with TBST for a total of 15 min, followed by incubation with goat antirabbit or antimouse IgG-horseradish peroxidase conjugates (1:2000) for 1 h at room temperature and four washes with TBST for a total of 1 h. The immunoblots were visualized by enhanced chemiluminescence.

Immunocytochemistry and Confocal Microscopy

Following treatment, LNCaP cells were fixed in 4% formaldehyde for 20 min before permeabilization with 0.1% Triton X-100 in PBS at room temperature for 15 min followed by incubation in 1% FBS (in PBS) for another 1 h. Cells were stained for endogenous PH domaincontaining proteins (Akt, PHLPP, ILK) by incubation with specific antibodies (1:300) overnight, followed by incubation with the Alexa Fluor 555-conjugated goat antirabbit or Alexa Fluor 488-conjugated goat antimouse IgG (1:500) at room temperature for 2 h. Both primary and secondary antibodies were diluted in incubation buffer containing 1% bovine serum albumin in PBS. The cells were washed in PBS after each step and mounted using VECTASHIELD mounting medium with 4′,6-diamidino-2-phenylindole (DAPI; Vector Laboratories Inc., Burlingame, CA). The slides were allowed to set for at least 4 h before confocal images were acquired using a Zeiss LSM 510 inverted confocal laser scanning microscope operated with Zeiss LSM 510 software. Image analysis was performed using ImageJ (NIH) software.

Co-immunoprecipitation of Akt-PHLPP Complexes

The Triton-soluble membrane fractions and cytosolic fractions were isolated as described previously.[25] Briefly, drug-treated cell pellets were lysed with cytosol buffer (50 mM HEPES pH7.4, 10 mM NaCl, 1 mM $MgCl_2$, 0.5 M EDTA, 1 mM phenylmethylsulfonyl fluoride, and 1 mM Na_3VO_4) and passed through a 26-gauge needle 10 times. After centrifugation, the supernatants were collected as the cytosolic fractions. Triton-soluble membrane fractions were extracted from membrane pellets by resuspension in Triton X-100-containing lysis buffer (50 mM Tris-HCl, pH 7.5, 150 mM NaCl, 1 mM EGTA, 10 mM $MgCl_2$, 0.5% Triton X-100, and protease inhibitor mixture) and passed through a 26-gauge needle 10 times. After centrifugation, the supernatants were collected as the Triton-soluble membrane fractions. For co-immunoprecipitation, the Triton-soluble membrane fractions were precleared with protein A/G agarose beads and then incubated overnight with anti-Akt-bound agarose beads (Santa Cruz Biotechnology). After brief centrifugation, the beads were collected and washed once with Triton X-100-containing lysis buffer, once with wash buffer 1 (50 mM Tris-HCl, pH7.5, 500 mM NaCl, 0.2% Triton X-100), and once with wash buffer 2 (10 mM Tris pH7.5, 0.2% Triton X-100). Immunoprecipitates were then eluted from the beads by adding sample buffer followed by boiling at 95 °C for 5 min and subjected to Western blot analysis.

Testing of in Vivo Efficacy of 3 and 20 in PC-3 Tumor-Bearing Nude Mice

Ectopic tumors were established in athymic nude mice by subcutaneous injection of PC-3 cells (1×10^6 cells/ mouse). The establishment and growth of tumors were monitored by direct measurement with calipers. Mice with established tumors (mean starting tumor volume, approximately 50 mm^3) were randomized to treatment groups ($n = 7$) in two different experiments. In the first, mice were treated once daily for 21 days by intraperitoneal injection with (a) **3** at 50 mg/kg body weight, (b) **20** at 50 mg/kg body weight, or (c) vehicle (physiological saline/polyethylene glycol 400/DMSO/ Tween 80; 65:20:10:5 by volume). In the second, mice were treated once daily for 21 days by oral gavage with (a) **3** at 100 mg/kg body weight, (b) **20** at 100 mg/kg body weight, or (c) vehicle (0.5% methylcellulose/0.1% Tween 80 [v/v] in sterile water). Tumor burdens in both experiments were determined weekly using calipers (tumor volume, $width^2 \times length \times 0.52$).

Statistical Analysis

In vitro experiments were performed using 3–6 replicates in each group. All in vitro experiments were carried out at least two times on different occasions. Differences between group means of tumor burden were analyzed for statistical significance using two-sided Student *t* tests. Differences were considered significant at $P < 0.05$.

Acknowledgments

This work was supported by NIH grant R01CA172576 (to C.S.C.).

ABBREVIATIONS USED

DAPI 4′,6-diamidino-2-phenylindole

IKK	inhibitor of nuclear factor κB kinase
ILK	integrin-linked kinase
K_d	the dissociation constant
MDM2	murine double minute 2
MTT	3-(4,5-dimethylthiazol-2-yl)-2,5-diphenyl-2*H*-tetrazolium bromide
PDK1	phosphoinositide-dependent kinase
PH	pleckstrin homology
PHLPP1	PH domain leucine-rich repeat protein phosphatase isoform 1
PIP_2	phosphatidylinositol (4,5)-bisphosphate
PIP_3	phosphatidylinositol (3,4,5)-trisphosphate
PTEN	phosphatase and tensin homologue
SPR	surface plasmon resonance

REFERENCES

1. Song MS, Salmena L, Pandolfi PP. The functions and regulation of the PTEN tumour suppressor. Nature Rev. Mol. Cell Biol. 2012; 13:283–296. [PubMed: 22473468]
2. Yap TA, Garrett MD, Walton MI, Raynaud F, de Bono JS, Workman P. Targeting the PI3K-AKT-mTOR pathway: progress, pitfalls, and promises. Curr. Opin. Pharmacol. 2008; 8:393–412. [PubMed: 18721898]
3. Cantley LC. The phosphoinositide 3-kinase pathway. Science. 2002; 296:1655–1657. [PubMed: 12040186]
4. Vivanco I, Sawyers CL. The phosphatidylinositol 3-Kinase AKT pathway in human cancer. Nature Rev. Cancer. 2002; 2:489–501. [PubMed: 12094235]
5. LoPiccolo J, Granville CA, Gills JJ, Dennis PA. Targeting Akt in cancer therapy. Anticancer Drugs. 2007; 18:861–874. [PubMed: 17667591]
6. Morrow JK, Du-Cuny L, Chen L, Meuillet EJ, Mash EA, Powis G, Zhang S. Recent development of anticancer therapeutics targeting Akt. Recent Pat. Anti-Cancer Drug Discovery. 2011; 6:146–159. [PubMed: 21110830]
7. Pal SK, Reckamp K, Yu H, Figlin RA. Akt inhibitors in clinical development for the treatment of cancer. Expert Opin. Invest. Drugs. 2010; 19:1355–1366.
8. Luo Y, Shoemaker AR, Liu X, Woods KW, Thomas SA, de Jong R, Han EK, Li T, Stoll VS, Powlas JA, Oleksijew A, Mitten MJ, Shi Y, Guan R, McGonigal TP, Klinghofer V, Johnson EF, Leverson JD, Bouska JJ, Mamo M, Smith RA, Gramling-Evans EE, Zinker BA, Mika AK, Nguyen PT, Oltersdorf T, Rosenberg SH, Li Q, Giranda VL. Potent and selective inhibitors of Akt kinases slow the progress of tumors in vivo. Mol. Cancer Ther. 2005; 4:977–986. [PubMed: 15956255]
9. Han EK, Leverson JD, McGonigal T, Shah OJ, Woods KW, Hunter T, Giranda VL, Luo Y. Akt inhibitor A-443654 induces rapid Akt Ser-473 phosphorylation independent of mTORC1 inhibition. Oncogene. 2007; 26:5655–5661. [PubMed: 17334390]
10. Rhodes N, Heerding DA, Duckett DR, Eberwein DJ, Knick VB, Lansing TJ, McConnell RT, Gilmer TM, Zhang SY, Robell K, Kahana JA, Geske RS, Kleymenova EV, Choudhry AE, Lai Z, Leber JD, Minthorn EA, Strum SL, Wood ER, Huang PS, Copeland RA, Kumar R. Characterization of an Akt kinase inhibitor with potent pharmacodynamic and antitumor activity. Cancer Res. 2008; 68:2366–2374. [PubMed: 18381444]

11. Toral-Barza L, Zhang WG, Huang X, McDonald LA, Salaski EJ, Barbieri LR, Ding WD, Krishnamurthy G, Hu YB, Lucas J, Bernan VS, Cai P, Levin JI, Mansour TS, Gibbons JJ, Abraham RT, Yu K. Discovery of lactoquinomycin and related pyranonaphthoquinones as potent and allosteric inhibitors of AKT/PKB: mechanistic involvement of AKT catalytic activation loop cysteines. Mol. Cancer Ther. 2007; 6:3028–3038. [PubMed: 17989320]
12. Salaski EJ, Krishnamurthy G, Ding WD, Yu K, Insaf SS, Eid C, Shim J, Levin JI, Tabei K, Toral-Barza L, Zhang WG, McDonald LA, Honores E, Hanna C, Yamashita A, Johnson B, Li Z, Laakso L, Powell D, Mansour TS. Pyranonaphthoquinone lactones: a new class of AKT selective kinase inhibitors alkylate a regulatory loop cysteine. J. Med. Chem. 2009; 52:2181–2184. [PubMed: 19309081]
13. Wu Z, Robinson RG, Fu S, Barnett SF, Defeo-Jones D, Jones RE, Kral AM, Huber HE, Kohl NE, Hartman GD, Bilodeau MT. Rapid assembly of diverse and potent allosteric Akt inhibitors. Bioorg. Med. Chem. Lett. 2008; 18:2211–2214. [PubMed: 18296048]
14. Barnett SF, Defeo-Jones D, Fu S, Hancock PJ, Haskell KM, Jones RE, Kahana JA, Kral AM, Leander K, Lee LL, Malinowski J, McAvoy EM, Nahas DD, Robinson RG, Huber HE. Identification and characterization of pleckstrin-homology-domain-dependent and isoenzyme-specific Akt inhibitors. Biochem. J. 2005; 385:399–408. [PubMed: 15456405]
15. Lindsley CW, Zhao Z, Leister WH, Robinson RG, Barnett SF, Defeo-Jones D, Jones RE, Hartman GD, Huff JR, Huber HE, Duggan ME. Allosteric Akt (PKB) inhibitors: discovery and SAR of isozyme selective inhibitors. Bioorg. Med. Chem. Lett. 2005; 15:761–764. [PubMed: 15664853]
16. Zhao Z, Leister WH, Robinson RG, Barnett SF, Defeo-Jones D, Jones RE, Hartman GD, Huff JR, Huber HE, Duggan ME, Lindsley CW. Discovery of 2,3,5-trisubstituted pyridine derivatives as potent Akt1 and Akt2 dual inhibitors. Bioorg. Med. Chem. Lett. 2005; 15:905–909. [PubMed: 15686884]
17. Mahadevan D, Powis G, Mash EA, George B, Gokhale VM, Zhang S, Shakalya K, Du-Cuny L, Berggren M, Ali MA, Jana U, Ihle N, Moses S, Franklin C, Narayan S, Shirahatti N, Meuillet E. Discovery of a novel class of AKT pleckstrin homology domain inhibitors. J. Mol. Cancer Ther. 2008; 7:2621–2632.
18. Du-Cuny L, Song Z, Moses S, Powis G, Mash EA, Meuillet EJ, Zhang S. Computational modeling of novel inhibitors targeting the Akt pleckstrin homology domain. Bioorg. Med. Chem. 2009; 17:6983–6992. [PubMed: 19734051]
19. Moses SA, Ali MA, Zuohe S, Du-Cuny L, Zhou LL, Lemos R, Ihle N, Skillman AG, Zhang S, Mash EA, Powis G, Meuillet EJ. In vitro and in vivo activity of novel small-molecule inhibitors targeting the pleckstrin homology domain of protein kinase B/AKT. Cancer Res. 2009; 69:5073–5081. [PubMed: 19491272]
20. Miao B, Skidan I, Yang J, Lugovskoy A, Reibarkh M, Long K, Brazell T, Durugkar KA, Maki J, Ramana CV, Schaffhausen B, Wagner G, Torchilin V, Yuan J, Degterev A. Small molecule inhibition of phosphatidylinositol-3,4,5-triphosphate (PIP3) binding to pleckstrin homology domains. Proc. Natl. Acad. Sci. U. S. A. 2010; 107:20126–20131. [PubMed: 21041639]
21. Meuillet EJ, Zuohe S, Lemos R, Ihle N, Kingston J, Watkins R, Moses SA, Zhang S, Du-Cuny L, Herbst R, Jacoby JJ, Zhou LL, Ahad AM, Mash EA, Kirkpatrick DL, Powis G. Molecular pharmacology and antitumor activity of PHT-427, a novel Akt/phosphatidylinositide-dependent protein kinase 1 pleckstrin homology domain inhibitor. Mol. Cancer Ther. 2010; 9:706–717. [PubMed: 20197390]
22. Kondapaka SB, Singh SS, Dasmahapatra GP, Sausville EA, Roy KK. Perifosine, a novel alkylphospholipid, inhibits protein kinase B activation. Mol. Cancer Ther. 2003; 2:1093–1103. [PubMed: 14617782]
23. Castillo SS, Brognard J, Petukhov PA, Zhang C, Tsurutani J, Granville CA, Li M, Jung M, West KA, Gills JG, Kozikowski AP, Dennis PA. Preferential inhibition of Akt and killing of Akt-dependent cancer cells by rationally designed phosphatidylinositol ether lipid analogues. Cancer Res. 2004; 64:2782–2792. [PubMed: 15087394]
24. Elrod HA, Lin YD, Yue P, Wang X, Lonial S, Khuri FR, Sun SY. The alkylphospholipid perifosine induces apoptosis of human lung cancer cells requiring inhibition of Akt and activation of the extrinsic apoptotic pathway. Mol. Cancer Ther. 2007; 6:2029–2038. [PubMed: 17604333]

25. Huang PH, Chuang HC, Chou CC, Wang H, Lee SL, Yang HC, Chiu HC, Kapuriya N, Wang D, Kulp SK, Chen CS. Vitamin E facilitates the inactivation of the kinase Akt by the phosphatase PHLPP1. Sci. Signaling. 2013; 6:ra19.

26. Gao T, Furnari F, Newton AC. PHLPP: a phosphatase that directly dephosphorylates Akt, promotes apoptosis, and suppresses tumor growth. Mol. Cell. 2005; 18:13–24. [PubMed: 15808505]

27. Brognard J, Sierecki E, Gao T, Newton AC. PHLPP and a second isoform, PHLPP2, differentially attenuate the amplitude of Akt signaling by regulating distinct Akt isoforms. Mol. Cell. 2007; 25:917–931. [PubMed: 17386267]

28. Mendoza MC, Blenis J. PHLPPing it off: phosphatases get in the Akt. Mol. Cell. 2007; 25:798–800. [PubMed: 17386258]

29. Chen M, Pratt CP, Zeeman ME, Schultz N, Taylor BS, O'Neill A, Castillo-Martin M, Nowak DG, Naguib A, Grace DM, Murn J, Navin N, Atwal GS, Sander C, Gerald WL, Cordon-Cardo C, Newton AC, Carver BS, Trotman LC. Identification of PHLPP1 as a tumor suppressor reveals the role of feedback activation in PTEN-mutant prostate cancer progression. Cancer Cell. 2011; 20:173–186. [PubMed: 21840483]

30. Lipinski CA, Lombardo F, Dominy BW, Feeney PJ. Experimental and computational approaches to estimate solubility and permeability in drug discovery and development settings. Adv. Drug Delivery Rev. 2001; 46:3–26.

31. Lasserre R, Guo XJ, Conchonaud F, Hamon Y, Hawchar O, Bernard AM, Soudja SM, Lenne PF, Rigneault H, Olive D, Bismuth G, Nunes JA, Payrastre B, Marguet D, He HT. Raft nanodomains contribute to Akt/PKB plasma membrane recruitment and activation. Nature Chem. Biol. 2008; 4:538–547. [PubMed: 18641634]

32. Gao X, Lowry PR, Zhou X, Depry C, Wei Z, Wong GW, Zhang J. PI3K/Akt signaling requires spatial compartmentalization in plasma membrane microdomains. Proc. Natl. Acad. Sci. U. S. A. 2011; 108:14509–14514. [PubMed: 21873248]

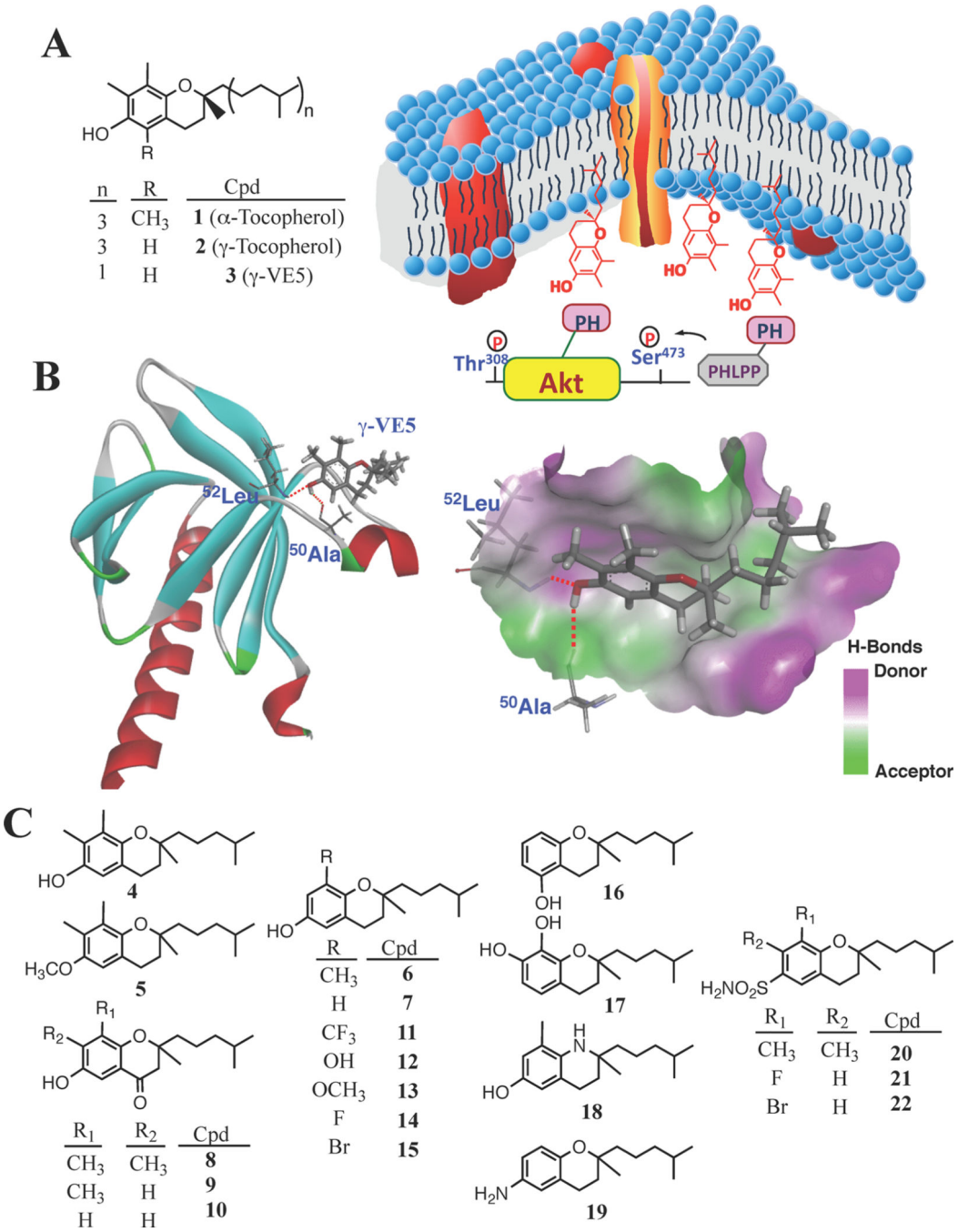

Figure 1.

γ-Tocopherol (**2**) as a scaffold to develop a novel class of PHLPP1-targeted Akt inhibitors. (A) Structures of **1, 2**, and **3** and a diagram depicting the unique mechanism by which **3** facilitates Ser473-specific Akt dephosphorylation through membrane co-localization of Akt and PHLPP1 in cancer cells. On the basis of docking of **3** into the VL2 loop of the Akt PH domain (PDB code, 1H10) (B), a series of analogues was synthesized (**4–22**) for biological evaluations (C).

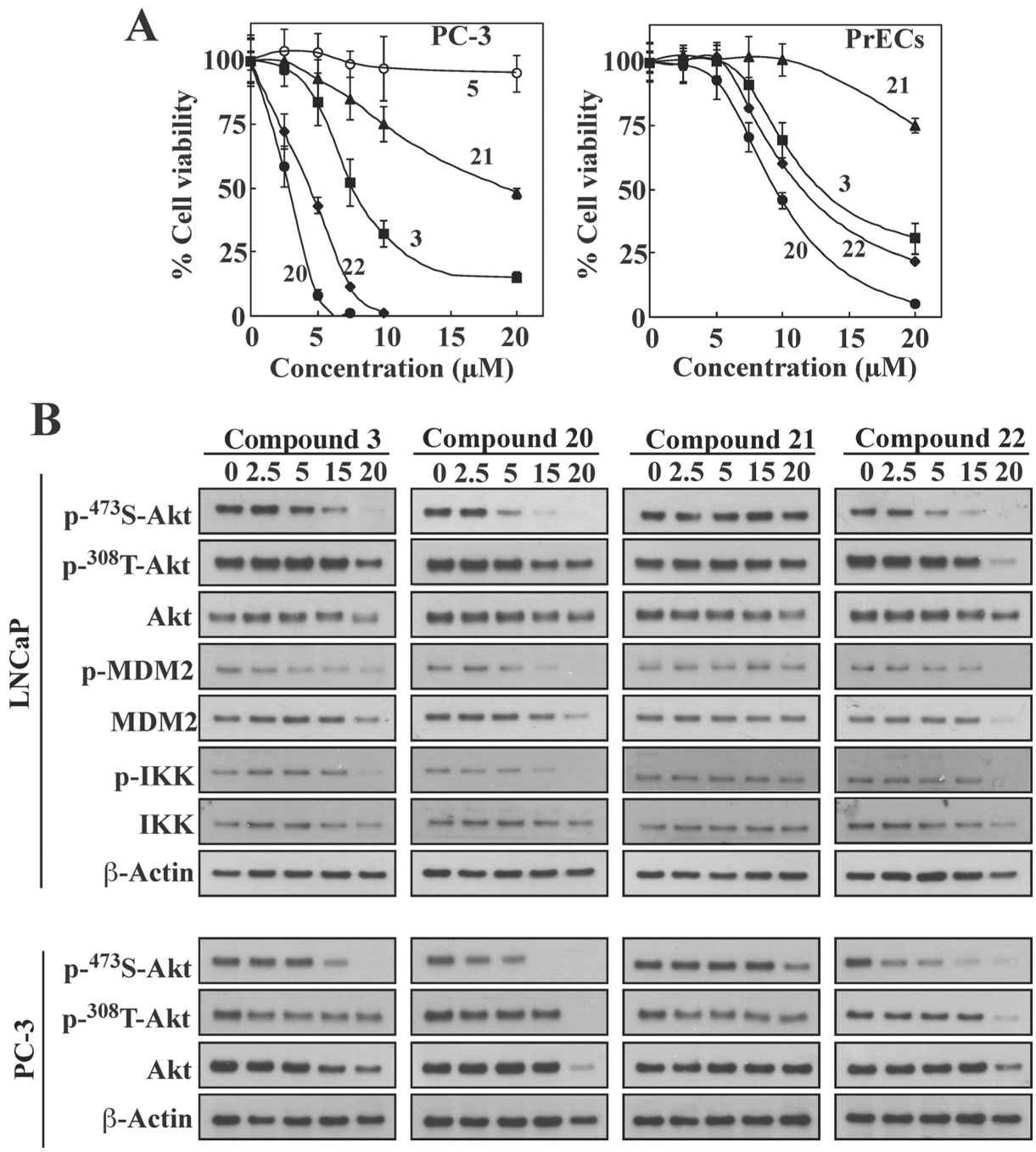

Figure 2.

Compounds **20** and **22** exhibit improved efficacy relative to **3** in suppressing cell viability and facilitating Akt inactivation in cancer cells. (A) Antiproliferative effects of **20, 21**, and **22** versus **3** were determined in PC-3 and PrEC cells by MTT assays following 24 h exposure in serum-free medium. Compound **5** was used as a negative control. Data are presented as means ± SD (n = 6). (B) Western blot analysis of the phosphorylation levels of Akt at Ser473 versus Thr308 and/or the downstream substrates MDM2 and IKK in LNCaP

(upper) and PC-3 (lower) cells exposed to different concentrations of individual agents for 24 h.

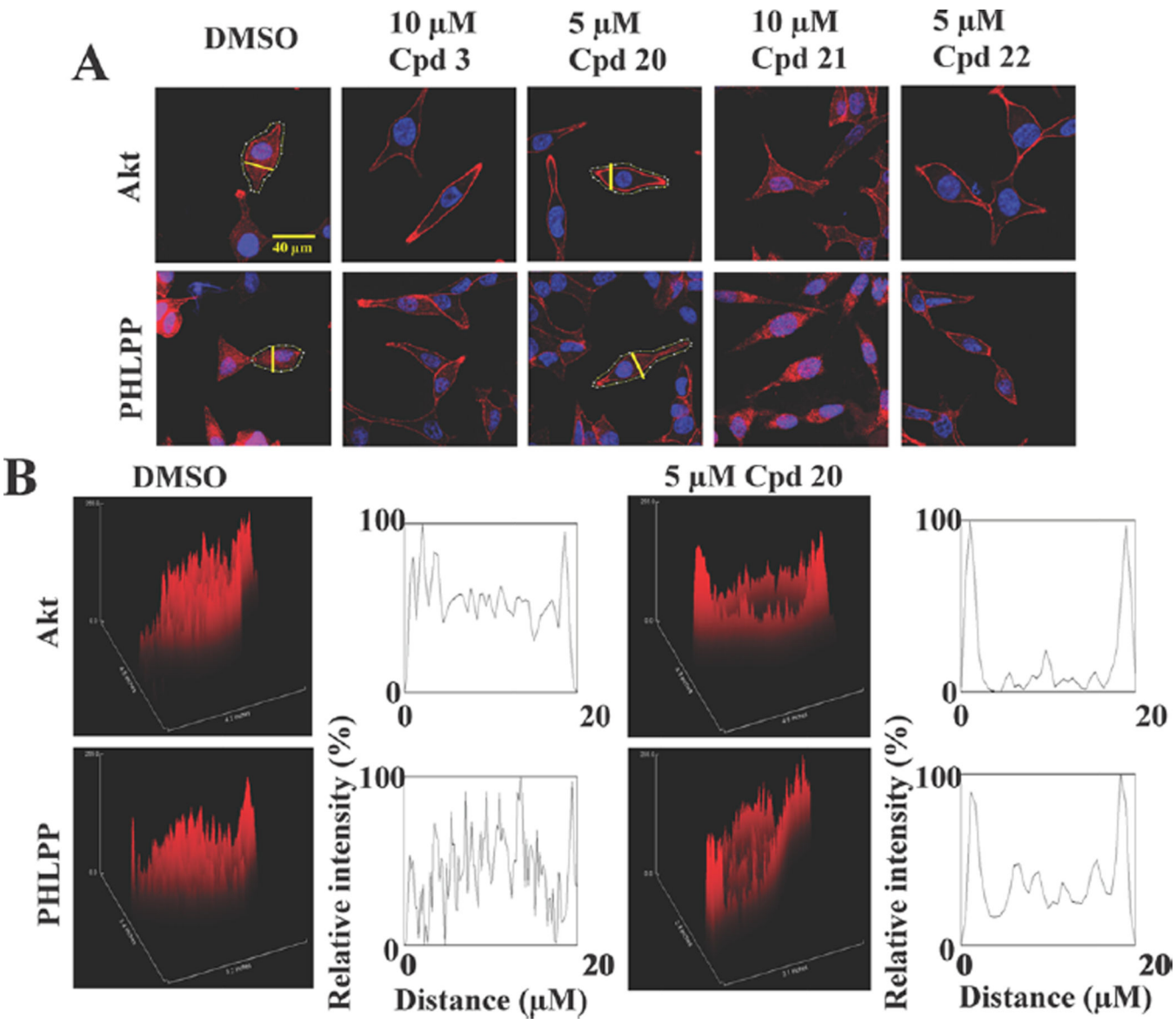

Figure 3.

Compounds **20** and **22**, but not **21**, share the ability of **3** to facilitate the translocation of Akt and PHLPP to the plasma membrane. (A) Immunofluorescence staining of Akt or PHLPP in LNCaP cells exposed to individual agents in serum-free medium for 24 h. Red, total Akt or PHLPP; blue, DAPI-stained nuclei. Yellow lines indicate the cross-sectional plane of analysis of fluorescence intensities in the following two-dimensional histograms. Scale bar, 40 μm. (B) Three-dimensional surface plots of fluorescence intensities of Akt and PHLPP1 in LNCaP cells treated with DMSO or 5 μM **20**, as shown above, and two-dimensional histograms of cross-sectional fluorescence intensities.

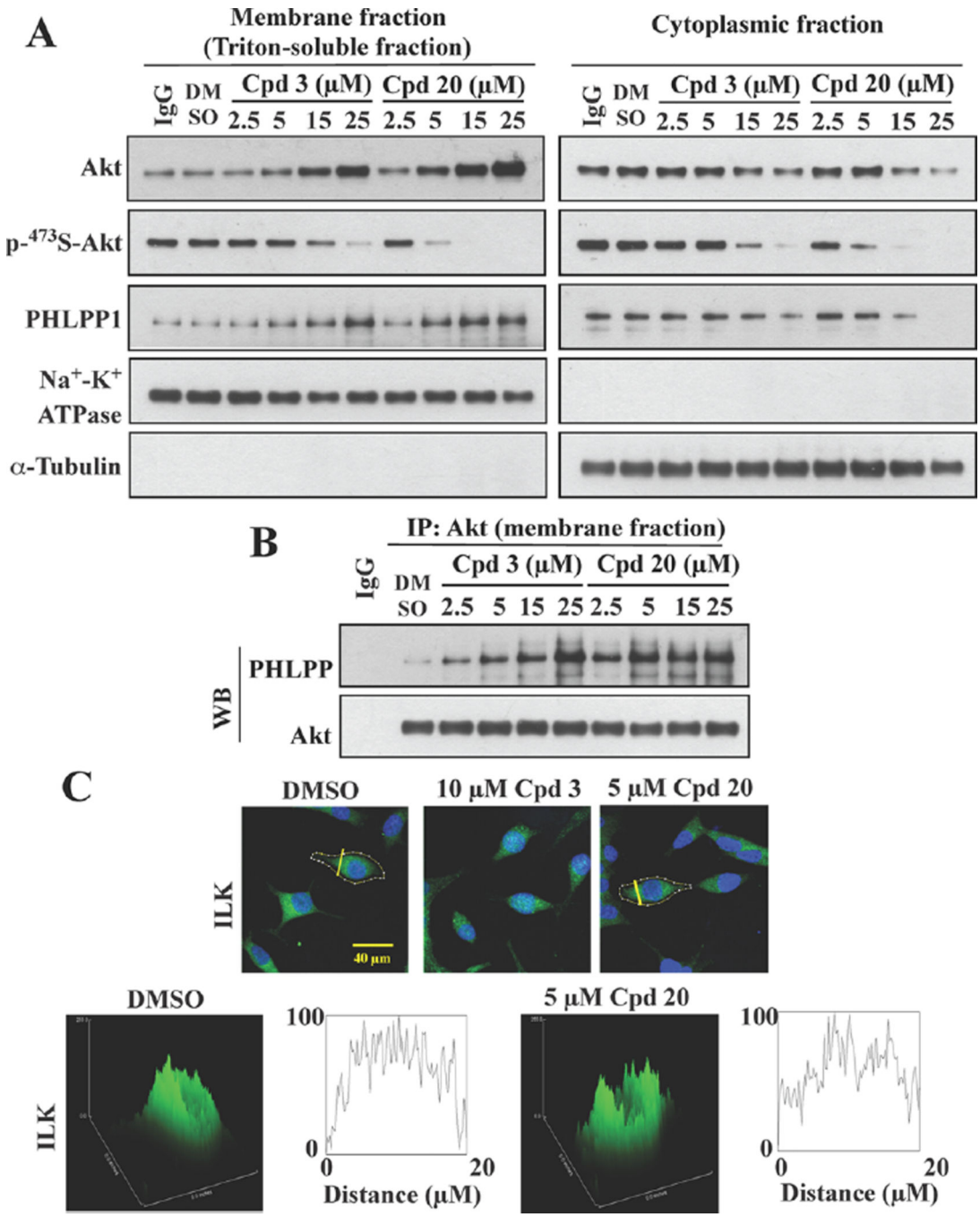

Figure 4.

Compound **20** facilitates the co-localization of Akt and PHLPP1 at the plasma membrane. (A) Western blot analysis of the levels of phospho-^{473}S-Akt, phospho-^{308}T-Akt, Akt, and PHLPP in the cytoplasmic and membrane fractions of LNCaP cells treated with **3** or **20** at indicated concentrations for 24 h, and (B) co-immunoprecipitation of Akt-PHLPP complexes from the membrane fractions described above. (C) Lack of effect of **3** and **20** on the cellular distribution of ILK, as indicated by immunofluorescence staining of ILK in

LNCaP cells exposed to **3** (10 μM) or **20** (5 μM) in serum-free medium for 24 h. Scale bar, 40 μm.

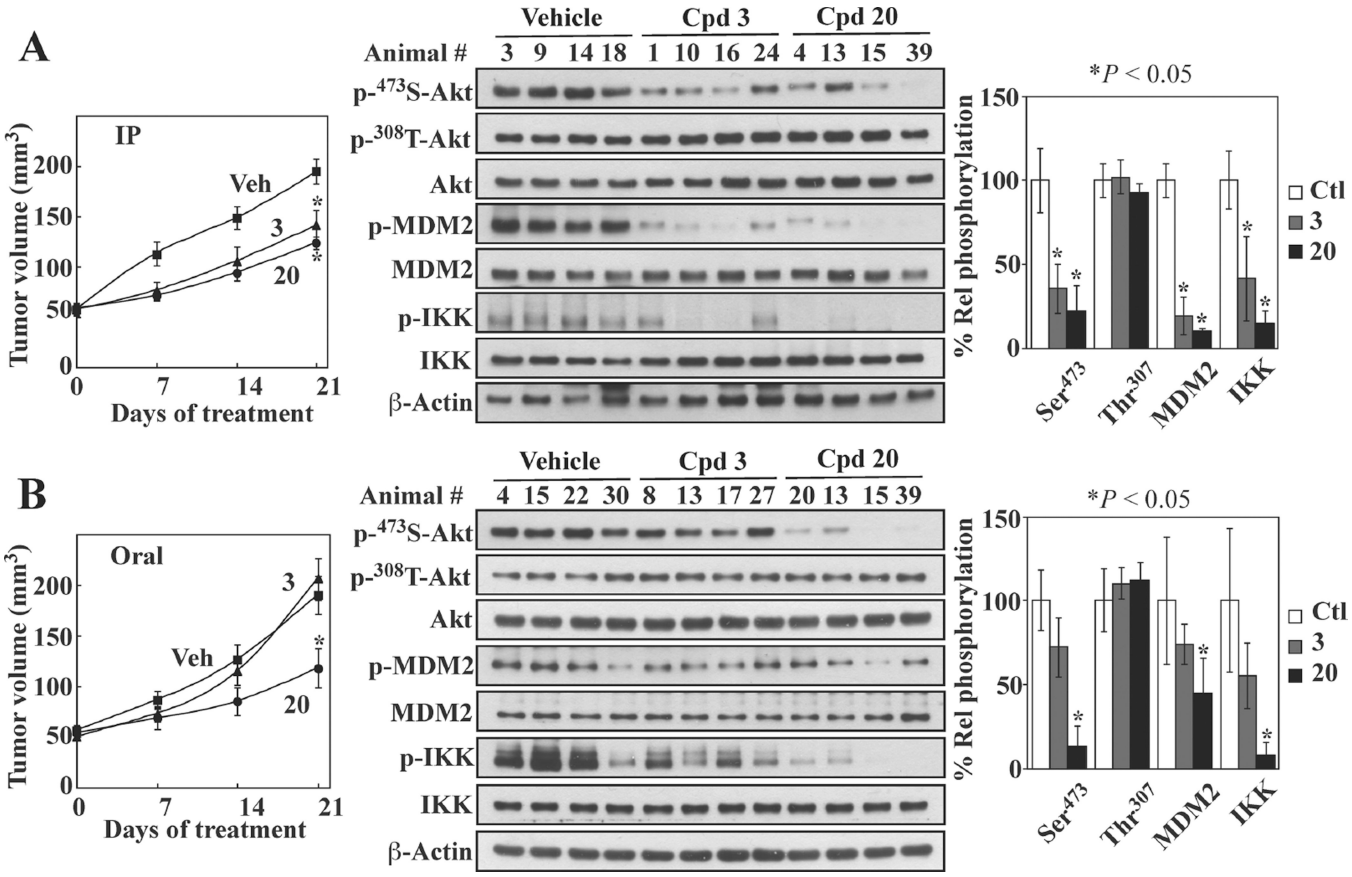

Figure 5.

In vivo efficacy of **20** vis-à-vis **3** in suppressing PC-3 xenograft tumor growth. Athymic nude mice bearing established subcutaneous PC-3 xenograft tumors were treated once daily with vehicle, **3**, or **20** via (A) ip injection at 50 mg/kg and (B) oral gavage at 100 mg/kg for 21 days. (left) Tumor volume data are presented as means ± SE (n = 7). (middle) Western blots of the phosphorylation of Ser473- versus Thr308-Akt, MDM2, and IKK in lysates from four representative tumors from each group of mice after 21 days of treatment. (right) Densitometric analysis of the Western blots showing suppressive effects of **20** and **3** on the phosphorylation of Ser473-Akt, MDM2, and IKK. Means ± SD (n = 4). *P < 0.05.

Table 1

Lipophilicities and Potencies of 3 and Individual Derivatives in Binding to the Akt PH Domain (K_d) and Suppressing the Viability of LNCaP Cells (IC_{50})

compd	calcd log *P*[a]	K_d (μM)[b]	IC_{50} (μM)[c]
2		ND[d]	>100
3	5.8	0.54 ± 0.24	7.5
4	5.8	0.52 ± 0.18	7.8
5	6.0	8.5 ± 2.7	>30
6	5.3	0.41 ± 0.12	7.5
7	4.8	0.35 ± 0.10	10
8	4.9	0.41 ± 0.18	10
9	4.1	0.32 ± 0.12	18
10	3.6	0.28 ± 0.10	>30
11	5.7	0.45 ± 0.07	8
12	4.6	1.18 ± 0.62	27
13	4.9	1.88 ± 0.46	26
14	5.0	0.34 ± 0.16	9
15	5.6	0.39 ± 0.12	8
16	4.8	0.34 ± 0.15	11
17	4.6	0.98 ± 0.3	23
18	5.1	0.03 ± 0.02	10
19	4.3	0.21 ± 0.07	>30
20	4.8	0.20 ± 0.08	3
21	4.0	0.35 ± 0.12	20
22	4.5	0.22 ± 0.10	4.5

[a] Calculated by Discovery Studio (Accelrys Software, San Diego, CA).

[b] Determined by SPR.

[c] Determined by MTT assays after 24 h of treatment in LNCaP cells.

[d] ND, could not be determined due to insolubility.

Table 2

Differential Binding Affinities of 3, 20, and 22 for the PH Domains of PHLPP1 versus PDK1 and ILK

	K_d (μM)		
	PHLPP1	**PDK1**	**ILK**
3	0.69 ± 0.36	10.2 ± 1.2	8.7 ± 3.6
20	0.72 ± 0.21	19.5 ± 4.9	6.2 ± 2.7
22	0.69 ± 0.12	11.1 ± 6.4	13.1 ± 3.6